1E3-3

Proceedings of Symposium on Ultrasonic Electronics, Vol. 37 (2016)

16-18 November, 2016

A Study for Ultrasonic Super Resolution Imaging Using Tissue Harmonics

Jing Zhu†, Shuntaro Hamazumi, Yihsin Ho, Kan Okubo and Norio Tagawa
(Graduate School of System Design, Tokyo Metropolitan University)

1. Introduction

Tissue Harmonic Imaging (THI) can provide medical ultrasound images of higher quality than fundamental imaging techniques. Because the THI can improve axial resolution due to higher frequencies and better lateral resolution due to narrower beams. However, the amplitude of the harmonic component is smaller than that of the fundamental component. Additionally, frequency dependent attenuation (FDA) is severe especially for the harmonic components. These phenomena lower the SNR of the THI.

In order to solve these THI problems, we have already proposed maximum a posteriori (MAP) estimation in Yamamura et al. [1] and an FDA compensating method in Hiraoka et al. [2]. In this study, for further high resolution, a Super resolution FM-Chirp correlation Method (SCM) in [3] is applied to the THI. The SCM is based on the MUSIC (MUltiple SIgnal Classification) algorithm introduced by Schmidt [4], which is proposed as a direction-of-arrival estimation method for electrical waves. The SCM can improve the range resolution of echoes by transmissting multiple pulses each having different frequency. The THI with the SCM is expected to have higher range resolution, but the influence of noise is a concern. We evaluate the effectiveness of the SCM for the THI through FEM simulations.

2. Method

SCM can achieve super-resolution imaging by utilizing the phase information of the carrier waves after compressing FM chirp echo signals. We obtain an analytic signal z consisting of an in-phase (I) component and a quadrature (Q) component from a compressed echo signal to calculate the covariance matrix R=E$\{zz^H\}$. From the eigenvalue equation

$$Re_i = \lambda_i e_i \quad : i = 1,2,...,M, \tag{1}$$

we can obtain the eigenvalues λ_i and the corresponding eigenvectors e_i (i=1,2,…, M), where M indicates the temporal sampling number of the echo. To estimate R by which different scatterers are distinguished finally, we define the following estimate using the analytic echo set $\{z(j)\}$ in which each $z(j)$ is measured by transmitting the pulse having different carrier frequency.

$$\hat{R} = \frac{1}{N}\sum_{j=1}^{N} z(j)z(j)^H . \tag{2}$$

When we arrange the M eigenvalues in descending order, the first D eigenvalues are large and the eigenvectors corresponding to $\{e_i\}_{i=1}^{D}$ span the signal subspace. D indicates the number of scatterers. On the other hand, a set of M-D eigenvalues λ_i (i = D+1,…,M) gets much smaller than those of $\{e_i\}_{i=1}^{D}$. The eigenvectors $\{e_i\}_{i=D+1}^{M}$ span the noise subspace.

In order to estimate the delay of the target's reflection, we use a measure of the orthogonality of the steering vectors to $\{e_i\}_{i=D+1}^{M}$. Accordingly, a super-resolution delay profile $S(\tau)$ based on the MUSIC algorithm can be defined as

$$S(\tau) = \frac{u(\tau)^H u(\tau)}{\sum_{i=D+1}^{M} \left| u(\tau)^H e_i \right|^2}, \tag{3}$$

where $u(\tau)$ denotes the delay profile vector for each delay τ. In actual applications, D should be determined using, for example, AIC and MDL.

In principle, the SCM method can apply to any reception signal, not just an FM-chirp signal. Especially in this study, to obtain a strong harmonic component, we use a short pulse having high intensity instead of an FM-chirp in [3].

3. Simulations

We confirmed the effectiveness of the proposed method through simulations using combination of PZFlex and SpectralFlex, those softwares are standard finite element method (FEM) simulator for ultrasound propagation. **Figure.1** show conditions used in the simulations. In this study, we use short pulses instead of FM-chirp long pulses as shown in Fig. 1(b). A transmitted pulse is emitted towards a wide range region, which is formed by a linear array transducer model with 96 elements, which is put at the left end of Fig. 1(a). Each element width and each separation is 0.13 mm and 0.01 mm respectively, and an aperture with a width of 13.44 mm is formed. A target object is located 15 mm away from the transducer in the area filled with water. Material properties used in the FEM simulations are given in **Table I**.

In the simulations, 15 pulses with randomly varying the center frequency from 4MHz to 6MHz were transmitted, and to verify the effectiveness of SCM using the synthetic aperture technique for the THI.

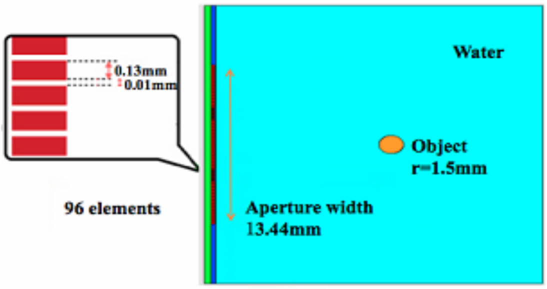

(a)

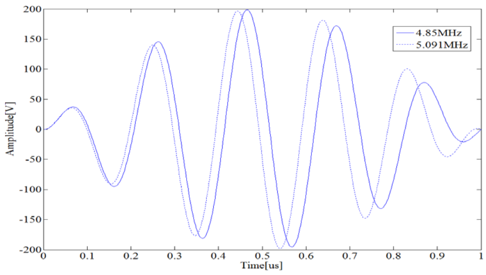

(b)

Fig. 1 Simulation conditions: (a) simulation model; (b) examples of transmitted signal;

Table I. Material properties used for FEM

Material	Density (kg/m3)	Velocity (m/s)	Attenuation coefficient (dB/cm/MHz)	Nonlinear parameter (B/A)	Distance (mm)
water	1000	1500	0.002	5	/
object	1080	1600	0.6	7	15

4. Results and Discussion

Figure.2 shows the received echo signal, and **Figure.3** shows the amplitude of the spectrum of it. Through the Fig. 3, it is confirmed that the second harmonic components were existed.

Figure.4 shows the result of SCM using the synthetic aperture. The fundamental envelop (red dotted line), the harmonic envelop (blue dashdot line), the fundamental SCM (black dashed line) and the harmonic SCM (green line) are indicated individually. All results are normalized and the figure indicates that the bandwidth of the SCM signal is sufficiently narrower then that of conventional signal. Furthermore, the harmonic SCM is narrower than the fundamental SCM, as their pulses width are 0.377 μs and 0.4 μs respectively.

5. Conclusion and Future Work

Through simulation, it is confirm that the THI range resolution is improved by adopting the SCM method. Therefore, the performance of the method was verified. However, in these results, the pulse width was not sufficiently narrow due to the interference between the fundamental and harmonic components. In the future work, we will solve this problem and aim to further a good estimation.

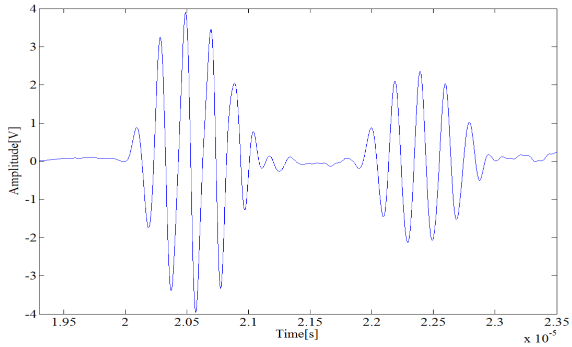

Fig. 2 Example of received echo signal.

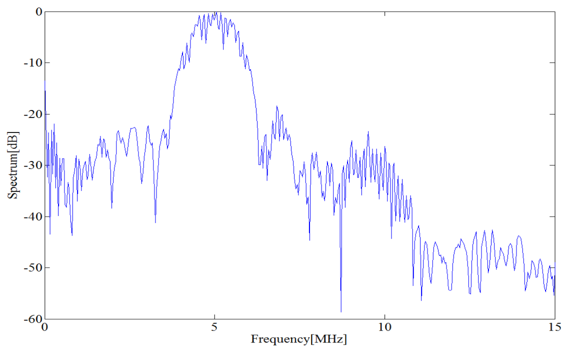

Fig. 3 Spectrum amplitude of received echo signal.

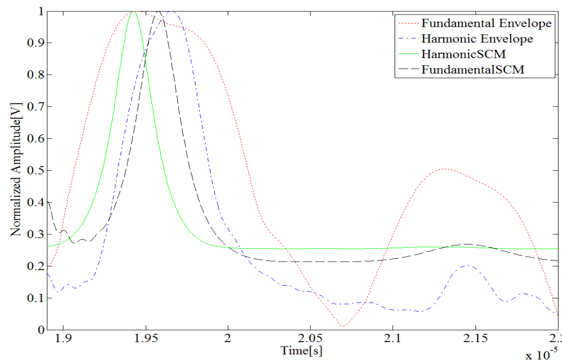

Fig.4 SCM results

References

1. T. Yamamura et al.: Japanese Journal of Applied Physics. 51 (2012) 07GF01.
2. T. Hiraoka and N. Tagawa: IEEE Int. Ultrasonics Symp. (2013) 914-917.
3. M.Fujiwara, K. Okubo and N. Tagawa: IEEE Int. Ultrasonics Symp. (2009) 2390-2393.
4. RO. Schmidt, IEEE Trans. Antennas and Propagation 34 (1986) 276-280.